

The superdeformed excited band of ^{40}Ca

E. Caurier ^a, F. Nowacki ^a, A. Poves ^b and A. Zuker ^a

(a) *IREs, Bât27, IN2P3-CNRS/Université Louis Pasteur BP 28, F-67037 Strasbourg Cedex 2, France*

(b) *Departamento de Física Teórica, C-XI. Universidad Autónoma de Madrid, E-28049, Madrid, Spain*

(Dated: December 11, 2018)

The superdeformed band, recently discovered in ^{40}Ca is analysed in an spherical shell model context. Two major oscillator shells, *sd* and *pf* are necessary to describe it. The yrast band of the fixed 8p-8h configuration fits extremely well with the experimental energies and transition rates of the superdeformed band. The 4p-4h configuration generates a normally deformed band plus a γ -band pattern which are also present in the experimental data.

PACS numbers: 21.10.Sf, 21.60.Cs, 23.20.Lv, 27.40.+z, 29.30.-h

The existence of excited deformed bands in spherical nuclei is a well documented fact, dating back to the 60's. A classical example is provided by the four particle four holes and eight particles eight holes states in ^{16}O , starting at 6.05 MeV and 16.75 MeV of excitation energy [1, 2]. However, it is only recently that similar bands, of deformed and even superdeformed character, have been discovered in other medium-light nuclei such as ^{56}Ni [3], ^{36}Ar [4] and ^{40}Ca [5] and explored up to high spin. These experiments have been possible thanks to the advent of large arrays of γ detectors, like Gammasphere or Euroball. One characteristic feature of these bands is that they belong to rather well defined spherical shell model configurations; for instance, the deformed excited band in ^{56}Ni can be associated with the configuration $(1f_{7/2})^{12} (2p_{3/2}, 1f_{5/2}, 2p_{1/2})^4$ while the (super)deformed band in ^{36}Ar has the structure $(sd)^{16} (pf)^4$. While many approaches are available for the microscopic description of these bands (Cranked Nilsson-Strutinsky, Cranked Hartree-Fock Bogolyubov, etc.) the interacting shell model is, when affordable, the prime choice. The mean field approach to $N=Z$ nuclei, has problems related to the proper treatment of the proton-neutron pairing in its isovector and isoscalar channels. On the shell model side, the problems come from the size of the valence spaces needed to accommodate the np-nh configurations, from the danger of center of mass contamination and from the occurrence of high level densities in the energy region where some of the members of the excited bands lay.

Prompted by our previous experience in the description of such states in ^{56}Ni and ^{36}Ar we have undertaken to explain the occurrence of deformed and superdeformed bands in ^{40}Ca as reported very recently by Gammasphere experimenters [5]. The states we aim to are dominantly core excitations from the *sd*-shell to the *pf*-shell. The natural valence space would thus comprise both major oscillator shells. However, the inclusion of the $1d_{5/2}$ orbit in the valence space produces a huge increase in the size of the basis and massive center of mass effects, thus we were forced to exclude it from the valence space already in the ^{36}Ar calculations and we will proceed equally

now, taking a closed core of ^{28}Si . We are aware that this truncation will somehow reduce, although not drastically, the quadrupole coherence of our solutions. Hence, our valence space will consist of the orbits $2s_{1/2}, 1d_{3/2}, 1f_{7/2}, 2p_{3/2}, 1f_{5/2}, 2p_{1/2}$. The effective interaction is the same used in ref. [4] denoted *sdpf.sm*. In a first step, we keep fixed the number of particles excited from the *sd* to the *pf* orbits. We surmise that the 4p-4h configurations are responsible for the band built on the first excited 0^+ state of ^{40}Ca at 3.352 MeV excitation energy and for some related states, while the superdeformed band pertains to the 8p-8h configurations. Indeed, the assumption of a fixed np-nh character for the states is not fully realistic, some mixing being always present. In spite of this, we believe that the np-nh states contain most of the physics relevant to the problem. In a second step we will deal explicitly with some features of the mixing.

TABLE I: Calculated γ energies for the 4p-4h configuration's yrast band and γ bands in ^{40}Ca , compared to the experimental bands labeled 2 and 4 in [5] (energies in keV)

$E_\gamma(J_i \rightarrow J_f)$		band 2	th. yrast	band 4	th. γ -band
2	0	553	772		
3	2			781	819
4	2	1375	1121	1260	1244
5	4			1369	1187
6	4	1653	1458		
7	5			1538	1501
8	6	2374	2210		
9	7			2773	2346
10	8	2381	2050		
11	9			1827	1518
12	10	2546	2866		
13	11			3044	1943
14	12	2297	1923		
16	14	4050	3374		

The γ -ray energies obtained in the diagonalizations in the 4p-4h space are gathered in table I and compared with the experimental results from [5]. The agreement is satisfactory. The most salient aspect of the calculated results is the triaxial character of the solution, with a well developed γ -band based in the second 2^+ state of the 4p-

4h configuration. The yrast sequence follows nicely the pattern of the experiment (Band 2 in [5]) within 200 keV, except for the highest spin member of the band, $J=16^+$, that comes out clearly too low. The experimental band presents an upbending at $J=10^+$, that the calculation turns out into a slight backbending. The calculated γ -band can be put in correspondence with the experimental states grouped in Band 4.

TABLE II: Quadrupole properties of the 4p-4h configuration's yrast-band in ^{40}Ca (in e^2fm^4 and efm^2)

J	B(E2)(J \rightarrow J-2)	Q_{spec}	$Q_0(\text{s})$	$Q_0(\text{t})$
2	266	-28.6	100	116
4	356	-39.9	110	112
6	328	-47.5	119	102
8	298	-42.3	101	96
10	220	-44.5	102	81
12	80	-38.6	87	94
14	111	-40.9	90	57
16	46	-34.7	76	37

The B(E2)'s and the quadrupole moments corresponding to the (4p-4h)-yrast states are presented in table II. The calculations assume harmonic oscillator single particle wave functions with size parameter $b=1.97$ fm, extracted from the experimental charge radius of ^{40}Ca . Effective charges $\delta e_\pi=\delta e_\nu=0.5$ are used. The intrinsic quadrupole moments behave quite regularly up to the backbending regime; from there on, there is not a real intrinsic state. This is manifest in the rapid decrease of the values $Q_0(\text{t})$ (the intrinsic quadrupole moment extracted from the B(E2)'s assuming $K=0$) and in the large difference between $Q_0(\text{t})$ and $Q_0(\text{s})$ (the intrinsic quadrupole moment extracted from the spectroscopic quadrupole moment, assuming $K=0$). In the experimental article, a value $Q_0(\text{t})=0.74\pm 0.14$ eb is obtained from the measured fractional Doppler shifts. Our values are somewhat larger but in reasonable agreement with this figure, that corresponds to $\beta=0.27$, a typical value for a normally deformed band. The quadrupole properties of the γ -band are gathered in table III. They are consistent with our picture of an triaxial rotor. Assuming $K=2$, we can extract also the intrinsic quadrupole moments, that keep approximately constant along the band. The oscillations are much larger than before reflecting a less well defined intrinsic state. Very strong $\Delta J=1$ E2 transitions are calculated between the lower states of the band. At higher spins, the $\Delta J=2$ transitions take over rapidly.

The natural continuation of this study would have been to compute the yrast band of the 8p-8h configuration in the same space and with the same interaction, aiming to the explanation of the experimental superdeformed band. However, the extremely large dimension of the basis ($\approx 10^9$) poses a serious problem. These dimensions are at present tractable with the new versions of the codes ANTOINE and NATHAN [6], but, to calculate the

TABLE III: Quadrupole properties of the 4p-4h configuration's γ -band in ^{40}Ca (in e^2fm^4 and efm^2)

J	B(E2)(J \rightarrow J-1)	B(E2)(J \rightarrow J-2)	Q_{spec}	$Q_0(\text{s})$
2			26.8	93
3	411	132	-0.3	-
4	440	210	-16.8	116
5	229	189	-25.4	110
6	177	189	-35.7	125
7	123	229	-35.7	110
8	50	189	-46.7	134
9	82	200	-35.3	95
10	43	169	-42.6	110
11	26	113	-46.3	116
12	29	6	-38.6	95
13	9	83	-40.9	98

complete band will demand a huge computational effort. Nevertheless, our experience in the pf -shell tells us that, to limit the maximum number of particles in the $1f_{5/2}$ and $2p_{1/2}$ to two, produces results that are already very close to the complete ones. The extra one-particle excitations contribute mainly to the quadrupole coherence while, the two-particle excitations improve the pairing content of the solutions. These are huge calculations too ($\text{dim} \approx 3 \times 10^8$) but nonetheless doable. We have carried out the calculations in the fixed 8p-8h configuration using the interaction *sdpf.sm*. The gamma-ray energies along the yrast sequence are compared to the experimental results (Band 1 in ref. [5]) in fig. 1 in the form of a backbending plot. The interaction reproduces very satisfactorily the experimental results. The only difference is the change of slope in the experimental curve at $J=10$, not reproduced by the calculation, that is probably an effect of the mixing. Notice that the experimental (and the predicted) bands are very regular, showing no backbending, contrary to the situation in ^{48}Cr [7]. Due to the presence of *sd* particles in pseudo-SU3 orbitals, the alignment process is pushed to higher angular momentum. In fact our calculations predict a slight backbending at $J=20$ and an unfavoured band termination at $J=22,24$.

In table IV we have collected the quadrupole properties. The Q_0 's extracted from the B(E2)'s and from the spectroscopic quadrupole moments are nearly equal and reasonably constant up to the backbending, supporting the existence of a robust intrinsic state. The calculated Q_0 of 172efm^2 is in perfect agreement with the experimental value $Q_0(\text{t})=1.80_{-0.29}^{+0.39}$, obtained from the fractional Doppler shifts. This experimental value corresponds to a deformation $\beta \sim 0.6$, i.e. to a superdeformed shape. The calculation predicts a slight decrease of the deformation with increasing J , while experimentally it seems to remain constant until the highest measured spin state ($J=16$). This departure may be due to the blocking of the $1d_{5/2}$ orbital. Despite that, the calculation at fix particle-hole number contains most of

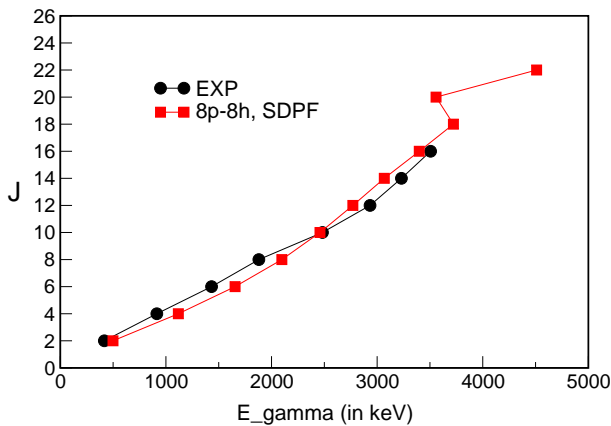


FIG. 1: The ^{40}Ca superdeformed band, experiment vs. the 8p-8h calculation in the sdpf valence space

the relevant physics of the superdeformed band in ^{40}Ca . The deformation that our calculation produces is probably the highest ever obtained in a shell model calculation describing a “bona fide” rotational band. As a matter of fact it almost saturates the SU(3) limit of the intrinsic quadrupole moment in these two major shells; $Q_0=190 \text{ efm}^2$, or the –more realistic– quasi-SU(3) one; $Q_0=180 \text{ efm}^2$. At the band termination, the $B(E2)$ ’s drop to zero while the spectroscopic quadrupole moments keep constant, reflecting the transition from the collective to the aligned regime.

TABLE IV: Quadrupole properties of the 8p-8h configuration’s yrast-band in ^{40}Ca , calculated in the *sdpf* valence space

J	$B(E2)(J \rightarrow J-2)$	Q_{spec}	$Q_0(t)$	$Q_0(s)$
2	589	-49.3	172	172
4	819	-62.4	170	172
6	869	-68.2	167	171
8	860	-70.9	162	168
10	823	-71.6	157	164
12	760	-71.3	160	160
14	677	-71.1	149	157
16	572	-72.2	128	158
18	432	-75.0	111	162
20	72	-85.1		
22	8	-79.1		
24	7	-81.5		

The next step is the study of the mixing of the different np-nh configurations. Unluckily, in this valence space, this goal is definitely beyond our computational possibilities –even with the truncation adopted above– because it demands the calculation of many states of the same total angular momentum. We try to circumvent these limitations by reducing once more the valence space, eliminating completely the upper *pf*-shell orbits. The active orbits will then be $2s_{1/2}$, $1d_{3/2}$, $1f_{7/2}$, $2p_{3/2}$. This valence space will be called *zbm2*, to emphasize its

links with the space $(1p_{1/2}, 1d_{5/2}, 2s_{1/2})$ used in the late 60’s to describe the core excited states of ^{16}O [8]. We have tried to evaluate the effects of this further truncation by comparing the 8p-8h results in the two spaces, with the interaction *sdpf.sm*. The the new γ -energies are presented in fig. 2 under the label *sm(1)*.

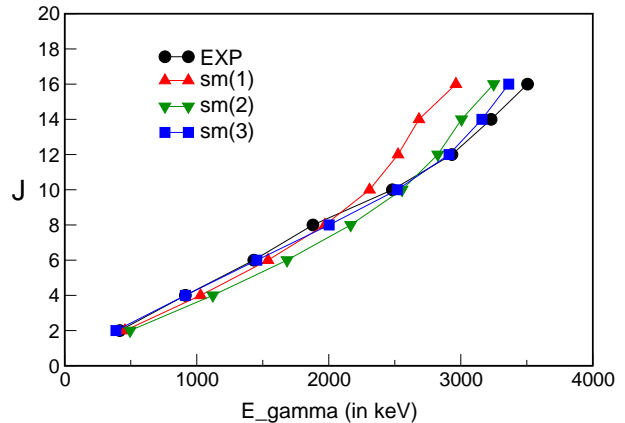


FIG. 2: The ^{40}Ca superdeformed band, experiment vs. different 8p-8h calculations in the *zbm2* valence space

The yrast band behaves nicely for the lower spins, but is too compressed beyond $J=10$. The quadrupole collectivity turns out to be a 10% smaller and decreases more rapidly at high spins than it does in the fuller calculation. This suggest that an increase of the quadrupole-quadrupole interaction in the *pf* sector of the interaction could mock the full space results. Therefore, we have increased a 10% the *qq* interaction and repeated the calculations in the *zbm2* space. The results for the energies are plotted in fig. 2 (label *sm(2)*), and we see that the band has now a much better behaviour and the correct span. However, the quadrupole properties remain basically unchanged. We have tried other interactions and/or renormalizations and our conclusion is that any decent interaction produces the same intrinsic state i.e. the quadrupole collectivity has reached saturation in this valence space. In order to increase the deformation and to keep it constant for the higher spins one must enlarge the valence space, this will increase the intrinsic quadrupole moment a 10% upon inclusion of the upper *pf*-shell and another 10% upon opening the $1d_{5/2}$ orbital. Thus, if we keep the usual effective charges, we have to be aware that the quadrupole coherence in the *zbm2* space will always be a 20% smaller than in the full space of the two major shells.

A new interaction has been built recently, specifically for the *zbm2* valence space, and used to describe the radii isotope shifts in the Calcium isotopes [9]. It was based on *sdpf.sm* with mostly monopole changes. Following our discussion above, we have increased a ten percent the quadrupole-quadrupole interaction in the *pf* sector of

the zbm2 space. In addition, in [9] an off-diagonal, cross-shell schematic isovector pairing was subtracted from the initial interaction to avoid double counting. Here we choose to reduce all the off-diagonal cross-shell matrix elements a 25%. It is with this interaction that we shall proceed to study the mixing. The results for the fixed 8p-8h configuration can be found also in fig. 2 with the label sm(3). As expected both the energies and the quadrupole properties are very close to the sm(2) set.

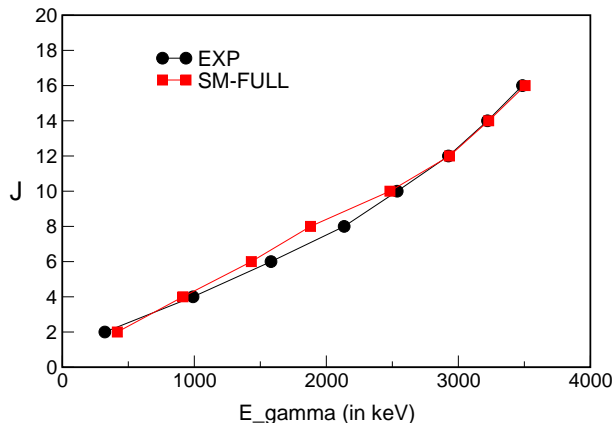


FIG. 3: The ^{40}Ca superdeformed band, experiment vs. mixed calculation in the full zbm2 space

The final step consists in finding the mixing among the different np-nh configurations. This is a formidable task because the np-nh series is not easy to truncate. In earlier studies [10] we have reached the conclusion that, in order to have the correct mixing in a given np-nh configuration, the valence space must contain at least all the configurations up to (np+4)-(nh+4). This is easy to understand, because the pairing interaction mixes configurations that are 2p-2h apart. But the amount of mixing depends also of their relative position, therefore, if the configurations that are 4p-4h apart are not included, the 2p-2h ones will be too high and will not renormalize the reference states properly. That's why the zbm2 valence space cannot provide the proper renormalization to the 8p-8h band, because the 10p-10h and 12p-12h configurations cannot develop enough collectivity due to the closure of the 1d5/2 orbit. This has two effects; first, as these configurations lay much too high in energy, they do not mix enough with the 8p-8h ones and the reduced gain in energy has to be compensated with an artificial lowering of the 8p-8h configurations. But even doing that, the absence of mixing with other configurations that have similar or larger quadrupole contents, makes the mixed results unphysically less collective than the unmixed ones. With all these caveats we have tried to get a first glimpse on the mixed results, that we comment now briefly. We have played freely with the *sd-pf* global monopoles in order to locate the three lower 0^+

states of ^{40}Ca close to their experimental values. The structure of the ground state is the expected one; about 60% closed shell, with mainly 2p-2h mixing. The first excited 0^+ is dominantly (60%) 4p-4h with mainly 6p-6h and 8p-8h mixing. It corresponds to the bandhead of the experimental Band 2. The third one is 60% 8p-8h, and the mixing is dominantly 4p-4h. The 10p-10h and 12p-12h component are –as we had anticipated– completely absent. The calculation of the three lower 0^+ is straightforward, however, the calculation of the excited states belonging to the 4p-4h or the 8p-8h bands is not, because these are most often drowned in a sea of other uninteresting states. To overcome this difficulty we select as starting vectors in the Lanczos procedure the eigenstates of the band obtained in the np-nh space. This choice accelerates the convergence of the states we are seeking and makes it possible to keep track of them in case of fragmentation. We have used this method to obtain the mixed superdeformed band, starting with the 8p-8h states. The excitation energies change little, but enough to improve the quality of the agreement with the experimental data of the 8p-8h calculation. (see figure 3). However, the quadrupole moments and transition probabilities get eroded –30% to 50%– by the mixing or even completely washed out at the top of the band. As we have discussed above, this is an intrinsic limitation of the valence space that we cannot overcome.

In conclusion we have performed a study of the many particle many hole configurations in ^{40}Ca , aiming to understand its recently discovered superdeformed excited band. We have shown that the yrast band of the 8p-8h configuration in the *sd-pf* valence space reproduces very well the experimental results and represents a show-case of superdeformed band described by the spherical shell model.

This work is partly supported by the IN2P3(France) CICyT(Spain) collaboration agreements. AP's work is supported by MCyT (Spain), grant BFM2000-30.

-
- [1] E. B. Carter, G. E. Mitchell and R. H. Davis, Phys. Rev. **133** 1421 (1964).
 - [2] P. Chevallier, F. Scheibling, G. Goldring, I. Plesser and M. W. Sachs, Phys. Rev. **16**+**0** 827 (1967).
 - [3] D. Rudolph, *et al.* Phys. Rev. Lett. **82**, 3763 (1999).
 - [4] C. E. Svensson, *et al.* Phys. Rev. Lett. **85**, 2693 (2000).
 - [5] E. Ideguchi, *et al.* Phys. Rev. Lett. **87**, 222501 (2001).
 - [6] E. Caurier, ANTOINE code, Strasbourg (1989-2002...), E. Caurier and F. Nowacki, Nathan code Strasbourg (1995-2002...)
 - [7] S. Lenzi, *et al.* Z. Phys. bf A354, 117 (1996).
 - [8] A. P. Zuker, B. Buck and J. B. McGrory, Phys. Rev. Lett. **21**, 39 (1968).
 - [9] E. Caurier, *et al.* Phys. Lett. B **87**, 240 (2001).
 - [10] A. Poves, J. Sánchez Solano, E. Caurier and F. Nowacki, to be published.